Quy-Huy TRIEU[1],
The-Thanh LUYEN[2],
Duc-Toan NGUYEN[3*]

OPTIMIZATION AND MODELLING OF FRACTURE HEIGHT IN SECC CYLINDRICAL CUP DEEP DRAWING PROCESSES

Deep drawing processes play a pivotal role in the manufacturing of sheet and shell products, making it a widely adopted method. This research employs numerical simulations to investigate the impact of various process parameters on the fracture height of cylindrical cups made from SECC (Steel Electrogalvanized Commercial Cold rolled) material. Specifically, it examines parameters such as blank holder force (*BHF*), punch corner radius (*Rp*), die corner radius (*Rd*), and punch-die clearance (*Wc*). The study extends to optimizing fracture height, offering a solution to this challenge. Subsequently, the selected parameters are validated through experimental deep drawing of cylindrical cups, resulting in a minimal deviation of 1.55% between simulation and experiment outcomes. A precise mathematical equation is developed to estimate fracture height under diverse machining conditions, with a maximum deviation of 4.52% observed between the mathematical model and simulation. These findings represent a substantial advancement in deep drawing processes technology, particularly in reducing error rates during the production of cylindrical cups.

1. INTRODUCTION

Deep drawing processes stand as a fundamental sheet metal forming technique that finds extensive application in industries such as automotive and related sectors. These processes entail the transformation of flat metal sheets into complex three-dimensional shapes, a task of paramount significance. However, the inherent complexities of deep drawing processes often lead to an array of challenges and defects, including rim wrinkling, cracks, and thinning of parts [1–4]. Correcting these issues demands a substantial investment of time and financial resources, along with a wealth of empirical experience. To address these challenges effectively, engineers and researchers have turned to computational tools, notably Finite Element Method (FEM) simulations. FEM simulations offer a means to not only enhance product quality but also to minimize production time by predicting defects before physical

_____

[1] Faculty of Mechanical Engineering, University of Economics - Technology for Industries, Hanoi City, Vietnam
[2] Faculty of Mechanical Engineering, Hungyen University of Technology and Education, Hungyen, Vietnam
[3] School of Mechanical Engineering, Hanoi University of Science and Technology, Hai Ba Trung District, Hanoi City, Vietnam
[*] E-mail:toan.nguyenduc@hust.edu.vn (D.T. Nguyen)

testing [5–8]. The ability to foresee and mitigate potential defects through simulation significantly reduces the incidence of flawed products, thus saving resources and curbing costly errors [9]. A plethora of studies in the realm of deep drawing processes has explored various facets of this critical manufacturing method. For instance, Müller and colleagues delved into the impact of process parameters, particularly the drawing ring radius, and process settings like multi-step and reverse deep drawing processes [10]. They applied their research to shaped cups manufactured from rectangular DP800 steel material. Mohsein and collaborators tackled the challenge of creating pentagonal cups using both numerical simulations and physical testing through two distinct methods [11]. The first approach involved converting a circular blank into a pentagonal cup through stamping, while the second method focused on reshaping a cylindrical cup into a pentagonal form. The evaluation of these two methods was grounded in parameters such as pressing force, stress/strain distribution, and thickness distribution of the pentagonal cup.

Li et al. [12] focused on the use of locally thick aluminum alloy plates for deep drawing processes square cups. Their study employed both numerical and experimental methods to assess various process parameters and the local sheet thickness's impact on the residual stress distribution in hot-deep drawing processes aluminum alloy square cups. The research illuminated that increasing the forming temperature, blank holder force, and die corner radius effectively reduced the residual stress in hot-deep drawing processes square cups. Chen et al. [13] explored the phenomenon of flange wrinkling under varying blank holder forces, employing AA1100-O material in their deep drawing processes experiments. Their study featured the development of a flange wrinkle reduction model, incorporating energy methods. This model facilitated the prediction of flange wrinkles by iteratively updating the flange's geometric parameters and material hardness in both simulation and experimental settings. Kardan et al. [14] delved into the effects of eight primary process parameters on deep drawing processes. These parameters encompassed punch and die radius, blank thickness, punch speed, blank holder force, lubrication conditions at the surfaces of the blank, and punch and blank holder configurations. The study deployed variance analysis to enhance the uniformity of deep drawing processes and product outcomes, revealing that punch/die corner radius, die specifications, and blank holder force (*BHF*) stood as the primary parameters influencing the deep drawing process force. Additionally, factors like workpiece thickness, die corner radius, and lubrication conditions at the contact surface exerted considerable influence on thickness distribution.

Modanloo et al [15] scrutinized the influence of deep drawing processes parameters on the required forming force, concentrating on copper/steel sheet composite materials. Utilizing the Taguchi method, they selected four parameters at three different levels and conducted experiments with a Taguchi L9 orthogonal array. Subsequently, they authenticated the maximum deep drawing force of each test through Finite Element (FE) modelling.

Agarwal et al. [16] ventured into deep drawing processes experiments employing TiAlN-coated molds, scrutinizing the effects of two distinct lubrication conditions. They amalgamated the L9 orthogonal array with input parameters such as lubrication, workpiece diameter, and forming speed, while output parameters encompassed forming force and height. Mrabti et al. [17] embarked on a study focusing on deep drawing processes applied to square profiles. Their research involved a combination of Analysis of Variance (ANOVA) and

process parameters such as punch/die corner radius, blank holder force (*BHF*), workpiece thickness, and three friction coefficients between the tool and workpiece. Tran et al. [18] introduced an innovative method for varying blank holder force, featuring a segmented blank holder, and examined its impact on surface roughness reduction in the circular deep drawing process of aluminum alloy plates. Their study incorporated analytical models and deep neural network (DNN) models, augmented by genetic algorithms (GA), for controlling *BHF*. The integrated DNN-GA model demonstrated precise prediction and optimization of diverse *BHF* configurations, particularly with regard to minimizing ear height variation, showcasing its superiority over analytical models.

As highlighted previously, significant deficiencies persist in the understanding and optimization of deep drawing methodologies, with a specific emphasis on the production of cylindrical cups. Through the integration of theoretical frameworks with practical applications, this research aims to provide concrete methodologies for enhancing the accuracy and efficacy of cylindrical cup manufacturing processes. Utilizing a combination of computational modelling and empirical validation, this approach seeks to develop a comprehensive framework capable of identifying key variables and optimizing their deployment. Consequently, the overarching objective is to streamline the manufacturing workflow, diminish the occurrence of errors, and reduce associated expenses in cylindrical cup production.

In this research, we embark on a comprehensive investigation that employs FEM simulations and experimental validation for deep drawing processes involving cylindrical cups fabricated from SECC (Steel Electrogalvanized Commercial Cold rolled) material. Our study scrutinizes pivotal process parameters, including blank holder force (*BHF*), punch corner radius (*Rp*), die corner radius (*Rd*), and punch-die clearance (*Wc*). We deploy the Taguchi orthogonal array and ANOVA variance method to assess the significance of these parameters in relation to fracture height in cylindrical cup production. Subsequently, we subject the selected parameters to rigorous validation through experimental deep drawing of cylindrical cups. Furthermore, we develop a highly precise mathematical equation tailored to estimate fracture height under a diverse array of machining conditions. These research outcomes signify a substantial contribution to the field of plate deep drawing processes, offering a promising avenue for reducing error rates during the production of cylindrical cups.

2. MATERIAL AND METHODS

In this section, we provide an overview of the materials used in the study, the mechanical properties, and the experimental and numerical methodologies employed to investigate the deep drawing processes.

2.1. MATERIAL SELECTION AND CHARACTERIZATION

The material under scrutiny in this research is SECC, characterized by a thickness of 0.6 mm. To accurately model the material behaviour, we adopted the Swift stress-strain model [19], as expressed by Equation (1):

$$\sigma_y = K(\varepsilon_0 + \bar{\varepsilon}^p)^n \qquad \text{with} \qquad \varepsilon_0 = \left(\frac{\sigma_0}{K}\right)^{1/n} \qquad (1)$$

Where: σ_y signifies the yield stress, $\bar{\varepsilon}^p$ denotes the equivalent strain; K, n and σ_0 are material parameters.
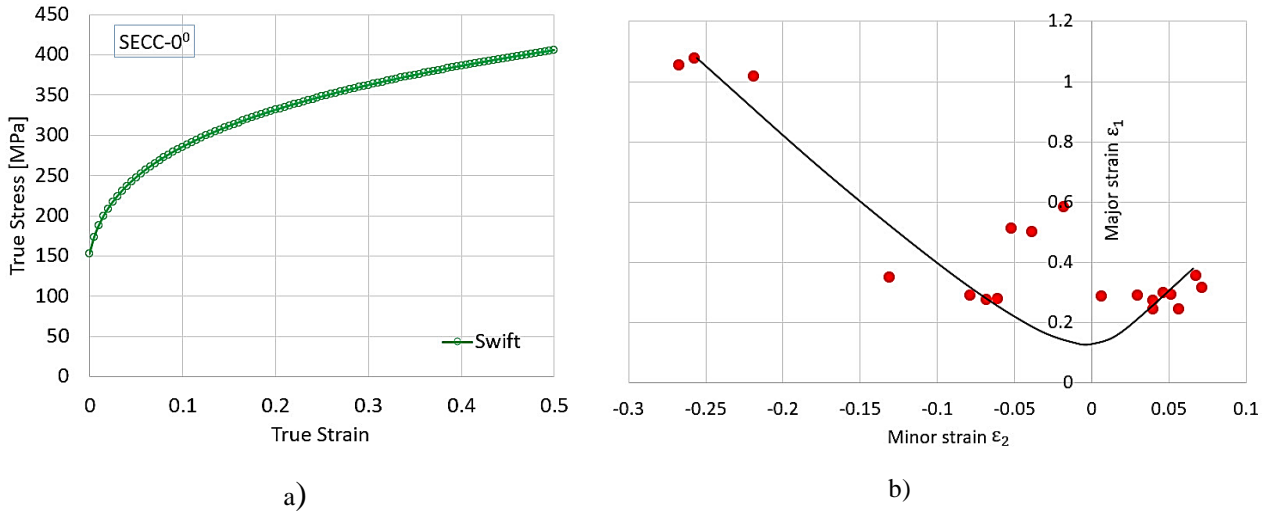

Fig. 1. The stress-strain curve-a) and Forming Limit Curve (FLC)-b) of SECC material

These material parameters (K, n and σ_0) were determined through uniaxial tensile tests conducted in the rolling direction, yielding the following values: $K = 473.5$ Mpa; $\sigma_0 = 152.5$ Mpa; $n = 0.226$. The material properties encompass density ($\rho = 7.85 \times 10^{-6}$ kg/mm^3), elastic modulus ($E = 184$ kN/mm^2), and Poisson's ratio ($v = 0.33$). Additionally, the anisotropy coefficient, determined via the Hill'48R model, will be further elucidated in the context of numerical simulations of cylindrical cup deep drawing processes. $R_{11} = R_{13} = R_{23} = 1$; $R_{22} = 1.0271$; $R_{33} = 1.1711$ and $R_{12} = 1.0968$) [20]. Figure 1a presents the stress-strain curve of SECC material and Figure 1b showcases the Forming Limit Curve (FLC) specific to SECC material used for the FEM simulation process.

2.2. FINITE ELEMENT (FE) SIMULATION MODEL

For the numerical investigation of deep drawing processes, we harnessed the computational power of ABAQUS 6.13 software [21]. The 3D FEM model, illustrated in Fig. 2b, embodies the geometric parameters of the die/punch set as depicted in Fig. 2a. This model featured a stationary punch while the die and the bank were mobile in the vertical direction. Absolute rigidity models were employed for the punch, die, and blank holder, with the sheet blank modelled using the S4R mesh. The friction coefficient between the punch and workpiece was set at 0.25, while the friction coefficient between the workpiece stop plate, deep punch, and the workpiece shared a value of 0.125 [22].
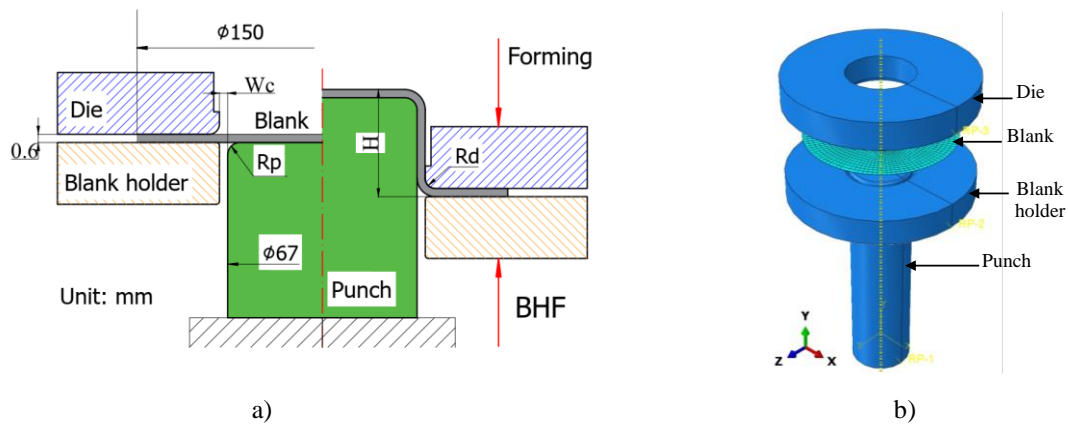
Fig. 2. The geometric parameters of the die/punch set - a) and 3D FEM model - b)

2.3. EXPERIMENTAL DEEP DRAWING PROCESSES

To validate the numerical simulations, experimental deep drawing processes were carried out using a 4-column dual hydraulic press model Y28-200. The workpiece had a diameter of Ø150 mm and a thickness of 0.6 mm. The deep drawing process mold consisted of key components, including the die, punch, and blank, as illustrated in Fig. 3. The die was affixed to the upper table of the hydraulic press and moved according to position sensor feedback. Conversely, the punch was secured to the lower machine table, and the blank holder's motion was controlled by the machine's lower hydraulic system. These components were manufactured from SKD11 material and underwent heat treatment. The mold's working surface exhibited a machined roughness of Ra = 0.63 μm. During the cylindrical cup deep drawing process, industrial oil was employed to mitigate friction between the mold components and the sheet blank.
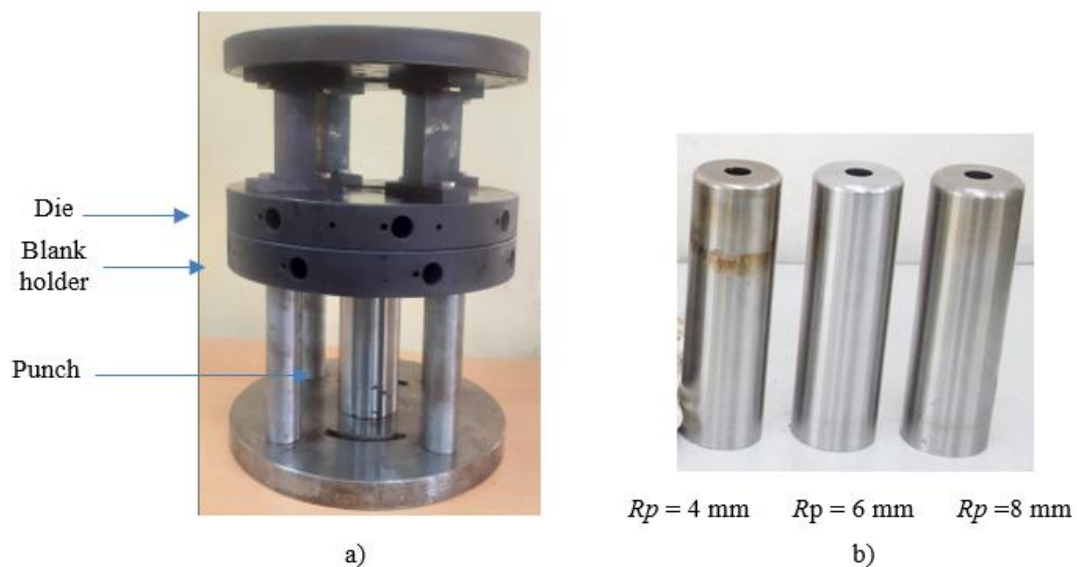

Fig. 3. The deep drawing process mold (a) and various punch of deep drawing processes (b)

2.4. ADDRESSING WRINKLING PHENOMENA

Wrinkles at the rim and tears at the punch corner often manifest during deep drawing processes. These issues arise due to misalignment between the mold's geometric parameters and the process's technological settings. Through the application of predefined boundary conditions during simulations, we sought to align the numerical and experimental outcomes to address these phenomena effectively. Wrinkle formation at the rim and tear occurrence at the cylindrical cup's corners were systematically observed during both simulation and experimentation, as depicted in Fig. 4a and 4b, respectively. As depicted in Fig. 4b, the occurrence of a tear enables the determination of the fracture height (H) of the cylindrical cup. To optimize the cylindrical cup's fracture height, we conducted a simulation-based parametric study according to Taguchi's experimental design, exploring variations in technological and geometric parameters such as blank holder force ($BHF = 10$–14 kN), punch corner radius ($Rp = 4 - 8$ mm), die corner radius ($Rd = 2$–6 mm), and punch-die clearance ($Wc = 0.8 \div 1.2$ mm). This rigorous investigation aimed to identify the most suitable parameters, validated through simulation and corresponding experimentation.
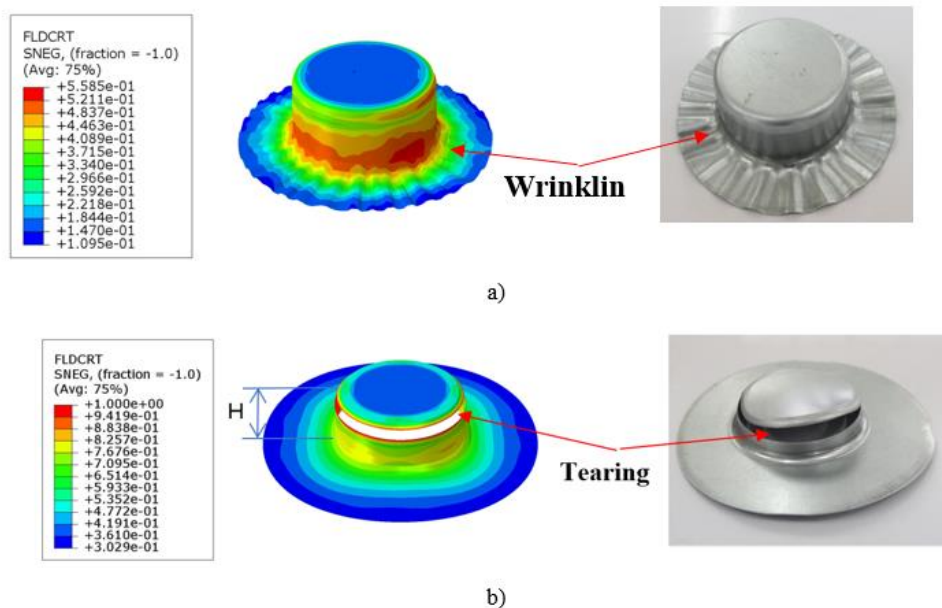

Fig. 4. Wrinkle formation at the rim - a) and tear occurrence at the cylindrical cup's corners - b) during both simulation and experimentation

3. RESULTS AND DISCUSSION

3.1. FACTORS IMPACTING FRACTURE HEIGHT AND IDENTIFICATION OF THE OPTIMAL PARAMETER SET

In this section, we present the results and discussion of our study, focusing on the influence of various process parameters on the fracture height (H) of cylindrical cups made

from SECC material. The key parameters considered include blank holder force (*BHF*), punch corner radius (*Rp*), die corner radius (*Rd*), and punch-die clearance (*Wc*). These parameters are fundamental to the deep drawing process, and their optimization is crucial for achieving the desired fracture height.

To systematically investigate these parameters, an experimental design following Taguchi's approach was adopted. This design allows for the efficient exploration of multiple factors at various levels while minimizing research time and costs. The specific parameter levels and corresponding values are summarized in Table 1:

Table 1. Input and output parameters

Parameters	Survey value domain	fracture height
Blank holder force (*BHF*)	10;12;14	
Punch conner radius (*Rp*)	4;6;8	*H* (mm)
Die conner radius (*Rd*)	2;4;6	
punch-die clearance (*Wc*)	0.8;1.0;1.2	

An orthogonal array (L9) was employed for conducting experiments, covering four factors (*BHF, Rp, Rd*, and *Wc*) with three levels each (Table 2). The experimental plans corresponding to the array L9 and three levels of four factors are presented in Table 3.

Table 2. Levels of influencing factors with corresponding values

	Factor	Level 1	Level 2	Level 3
	BHF (KN)	10	12	14
	R_p (mm)	4	6	8
Value	R_d (mm)	2	4	6
	W_c (mm)	0.8	1.0	1.2

The results obtained from the simulations were analysed using the signal-to-noise ratio (*S/N*) metric, which provides insights into the influence of input factors on the objective function, in this case, fracture height (*H*). The *S/N* ratio is calculated using various formulas depending on the desired outcome (larger is better, normal is best, or smaller is better).

The calculated *S/N* ratios for each test case are presented in Table 3 (as Eq. (2)), along with the corresponding fracture height values. To determine the influence of factors, an analysis of variance (ANOVA) was conducted. This analysis assesses the contribution of each factor to variations in fracture height.

$$S/N = -10 \log\left(\frac{1}{n}\sum\frac{1}{y_i^2}\right) \tag{2}$$

Where y_i represents the measured value from the i-th trial, averaged over multiple measurements taken in that particular trial. Meanwhile, *n* refers to the total number of tests or testing procedures performed. Fig. 5. Illustrates the fracture height of cylindrical cups

resulting from different parameter combinations during the simulation of the deep drawing process.

Table 3. Simulated fracture height results and corresponding *s/n* ratio values

Case No.	BHF (kN)	Rp (mm)	Rd (mm)	Wc (mm)	H_S (mm)	S/N
		Level				
1	10	4	2	0.8	34.25	30.693
2	10	6	4	1.0	44.12	32.893
3	10	8	6	1.2	45.86	33.229
4	12	4	4	1.2	31.68	30.016
5	12	6	6	0.8	40.18	32.080
6	12	8	2	1.0	34.89	30.854
7	14	4	6	1.0	33.67	30.545
8	14	6	2	1.2	26.78	28.556
9	14	8	4	0.8	33.88	30.599

The ANOVA results pertaining to fracture height (*H*) are succinctly presented in Table 4. This table encompasses several crucial elements, such as the Signal-to-Noise (S/N) ratio for each level, the summation of squares, contribution percentages, and the optimal factor values. These results serve as the foundation for determining the extent of influence each factor exerts. The influence levels of these factors are ascertained through the utilization of calculation formulas, as expressed in Equations (3) and (4).

$$m_{ji} = \frac{1}{3}\sum_{i=1}^{3}\left((S/N)_j\right)_i. \tag{3}$$

$$CF = \frac{T^2}{n} \tag{4a}$$

$$T = \sum_{i=1}^{n} Y_i \tag{4b}$$

$$S_j = \sum_{i=1}^{n_{ji}} \frac{j_i^2}{n_{ji}} - CF \tag{4c}$$

$$S_T = \sum_{j=1}^{n} S_j. \tag{4d}$$

$$P_j = \frac{S_j}{S_T} \tag{4e}$$

Where: m_{ji} represents the average of the noise ratios associated with each level i (where i can be 1, 2, or 3), with j designating the influencing parameters (typically denoted as A, B, or C); Y_i signifies the measurement outcome obtained during the i-th test condition. It is an average derived from multiple measurements conducted within that specific test; *n* corresponds to the total number of trials undertaken; n_{ji} represents the number of trials involving factor *j* at level *I*; *ji* indicates the cumulative result of factor *j* at level *i*. These factors collectively contribute to a comprehensive assessment of the experimental data and the determination of each factor's influence on fracture height.
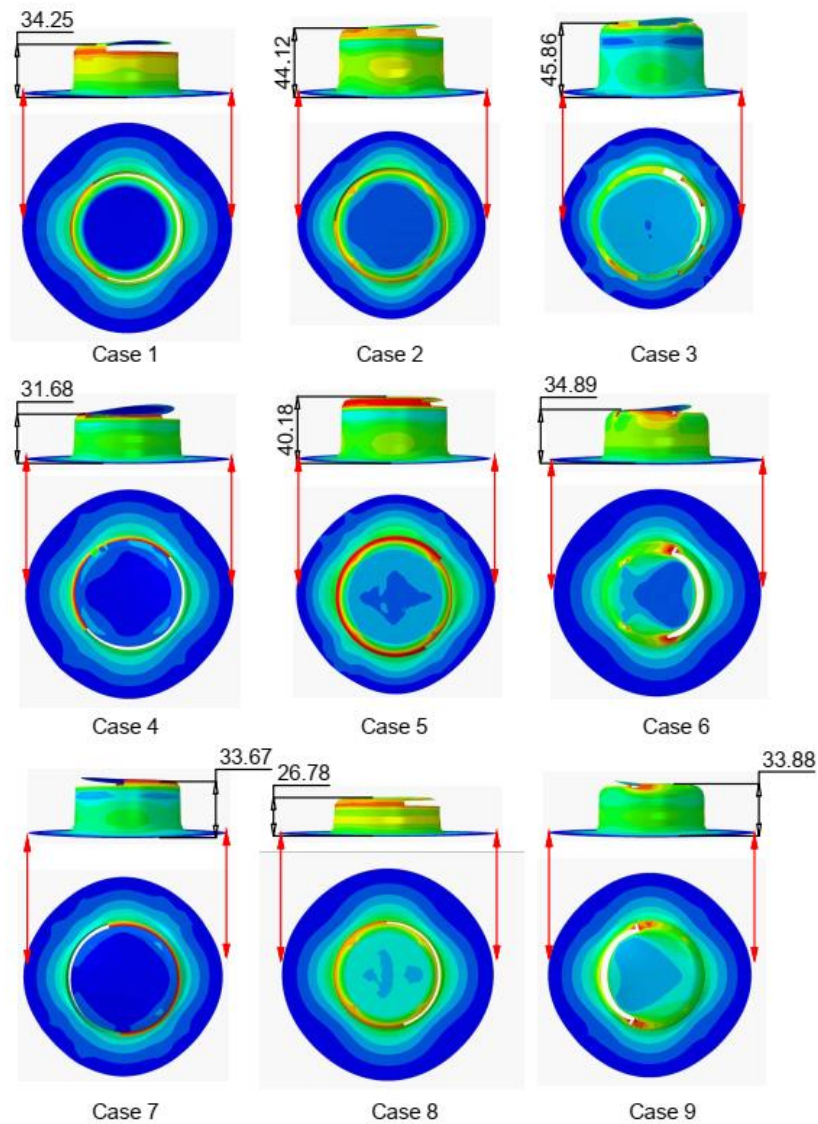
Fig. 5. Deformed shape and gracture height of L9's cylindrical cups

Table 4. ANOVA results for fracture height

Factor	The S/N ratio of each level			Sum of squares	Contribution (%)
	1	2	3		
A	32.272*	30.983	29.900	8.457	49.4
B	30.418	31.176	31.561*	2.028	11.9
C	30.034	31.169	31.951*	5.573	32.6
D	31.124	31.431*	30.600	1.058	6.2
Total				17.117	100.0

Figure 6 showcases the *S/N* ratio results for each parameter affecting fracture height (*H*). It provides a visual representation of the factors' influence levels on the objective function.
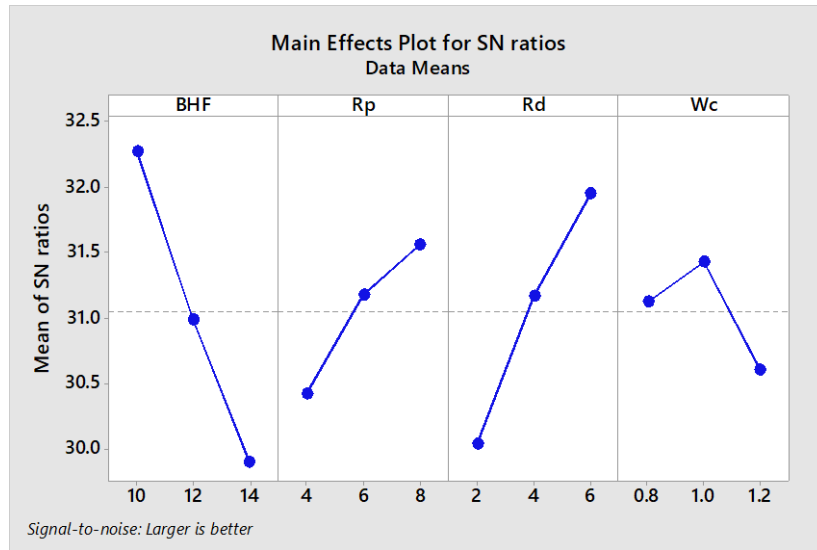
Fig. 6. S/N ratio results for each parameter affecting fracture height (*H*)

To assess the appropriateness of the selected parameters, the study calculated the percentage difference between the simulated and experimental fracture heights using Equation (5). The optimal parameter set that achieved the minimal deviation between simulation and experiment (1.55%) consists of *BHF* = 10 kN, *Rp* = 8 mm, *Rd* = 6 mm, and *Wc* = 1.0 mm.

$$\Delta H(\%) = (|H_s - H_E|)/H_E \tag{5}$$

Figure 7 displays the simulation and experimental results for the optimal parameter set, showcasing the fracture height of the cylindrical cup. The minimal difference of 1.55% between simulation (H_s = 50.28 mm) and experiment (H_E = 49.50 mm) demonstrates the effectiveness of the optimized parameters in achieving the desired fracture height.
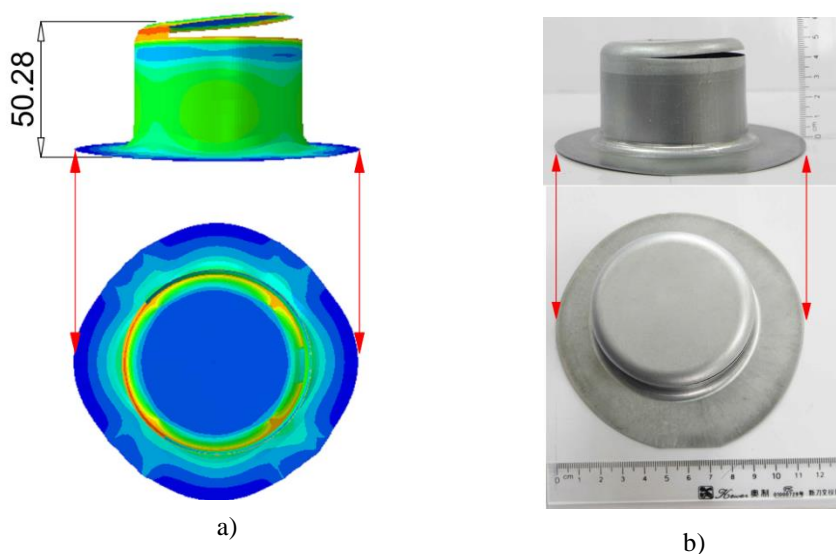

Fig. 7. Simulation – a) and experimental – b) results for the optimal parameter set

In summary, this comprehensive analysis of the deep drawing process parameters has provided valuable insights into optimizing fracture height, with a focus on *BHF*, *Rp*, *Rd*, and *Wc*. The findings emphasize the significant influence of *BHF* on fracture height, followed by *Rd*, while *Rp* and *Wc* exhibited relatively minor effects. This research contributes significantly to the advancement of deep drawing processes, particularly in reducing error rates during cylindrical cup production.

3.2. DEVELOPMENT OF THE MATHEMATICAL MODEL FOR FRACTURE HEIGHT IN CYLINDRICAL CUP DEEP DRAWING PROCESSES

The fracture height of a cylindrical cup is contingent upon several crucial parameters, namely, Blank Holder Force (*BHF*), Punch Corner Radius (*Rp*), Die Corner Radius (*Rd*), and Punch-Die Clearance (*Wc*). To establish a mathematical relationship between these four parameters and the target function, which is the fracture height (H_M) of the cylindrical cup product, we aim to analyze the trends and evaluate the impact of these parameters on the desired outcome. This mathematical relationship is expressed as Equation 6:

$$H_M = a \cdot BHF^b \cdot Rp^c \cdot Rd^d \cdot Wc^e \tag{6}$$

Here, *a, b, c, d,* and *e* represent the coefficients and exponents in Equation 6.

To construct a model for the fracture height in the deep drawing processes of cylindrical cups, we employ the Gauss-Newton nonlinear regression method. This method is implemented using the Nonlinear Regression tool within the Minitab 17 software. Input data is derived from the results of experiments conducted with an orthogonal array L9, as presented in Table 4. With nine experimental datasets, the coefficient and exponent values are determined as follows: *a = 151.306; b = –0.815; c = 0.186; d = 0.192; e = –0.138.*

To assess the reliability of the regression function (Equation 6), an ANOVA (Analysis of Variance) analysis is performed using Matlab. The results are summarized in Table 5:

Table 5. ANOVA analysis of variance table for factors influencing fracture height

Symbols	Degrees of freedom	Residual variance (S_u^2)	Repeated Variance (S_{ll}^2)	R^2	$F = \frac{S_u^2}{S_{ll}^2}$	$F_{0.05}$
BHF	2					
Rp	2					
Rd	2	3.825	1.816	0.982	2.106	9.01
Wc	2					
Total	8					

From the ANOVA table, it is evident that the regression coefficient $R^2 = 0.982$, and the coefficient $F = 2.106$ (theoretical) is less than 9.01 (table coefficient according to the Fisher standard). This indicates the high reliability of Equation 6.

To further validate the reliability of the nonlinear regression function model for fracture height of cylindrical cups, the study calculates the fracture height values based on the regression equation and compares them to simulated fracture heights, as depicted in Fig. 8. The results demonstrate that the largest deviation is 4.52%. Consequently, the mathematical model developed for determining fracture height in deep drawing processes exhibits a high degree of reliability.
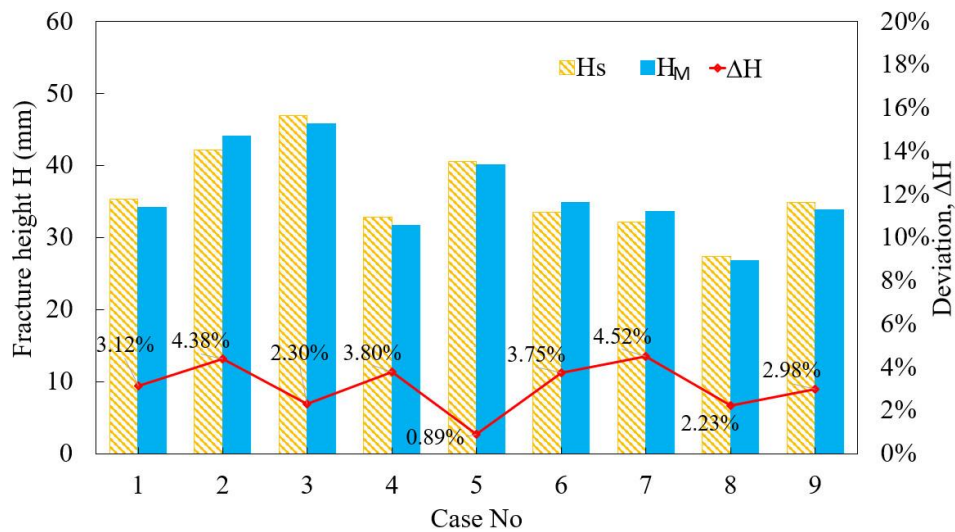

Fig. 8. Deviation in fracture height between mathematical model and simulation data

4. CONCLUSIONS

This study was undertaken to explore the influence of technological and geometric parameters on fracture height in the deep drawing processes of SECC cylindrical cup products. Through a comprehensive approach encompassing simulation, experimentation, and mathematical model development, several critical findings have been ascertained:

- Optimization of the deep drawing process has revealed that the parameter Blank Holder Force (*BHF*) exerts the most significant influence, accounting for 49.4% of the variance in fracture height. Subsequently, Die Corner Radius (*Rd*) demonstrates a lower influence at 32.6%. Punch Corner Radius (*Rp*) and Punch-Die Clearance (*Wc*) exhibit negligible effects on fracture height, contributing only 11.9% and 6.2%, respectively.
- The optimal parameter combination, denoted as A1B3C3D2 (comprising *BHF* = 10 kN, *Rp* = 8 mm, *Rd* = 6 mm, and *Wc* = 1.0 mm), was determined to achieve the maximum fracture height. Simulations and experimental verification corroborated this parameter set, yielding a deviation of a mere 1.55%.
- A robust mathematical model has been established to describe the relationship between input process parameters (*BHF*, *Rp*, *Rd*, and *Wc*) and fracture height (*H*) of cylindrical cups. The results underscore the model's reliability, with a maximum deviation of 4.52% between the mathematical model and simulation outcomes. This affirms the high fidelity of the mathematical model in predicting fracture height in deep drawing processes.

REFERENCES

[1] DAL S.R., DARENDELILER H., 2022, *Analysis of Side-Wall Wrinkling in Deep Drawing Processes*, Key Engineering Materials 926/12, 732-743, https://doi.org/10.4028/p-i5q886.

[2] LUYEN T.T., MAC T.B., BANH T.L., NGUYEN D.T., 2023, *Investigating the Impact of Yield Criteria and Process Parameters on Fracture Height of Cylindrical Cups in the Deep Drawing Process of SPCC Sheet Steel*, Int. J. Adv. Manuf. Technol., 0123456789, https://doi.org/10.1007/s00170-023-12022-8.

[3] LUYEN T., TONG V., NGUYEN D., 2021, *A Simulation and Experimental Study on the Deep Drawing Process of SPCC Sheet Using the Graphical Method*, Alexandria Eng. J., https://doi.org/10.1016/j.aej.2021.07.009.

[4] LUYEN T.T., NGUYEN D.T., 2023, *Improved Uniformity in Cylindrical Cup Wall Thickness at Elevated Temperatures Using Deep Drawing Process for SPCC Sheet Steel*, J., Brazilian Soc. Mech. Sci. Eng., 45/7, https://doi.org/10.1007/s40430-023-04270-2.

[5] BALLIKAYA H., SAVAS V., OZAY C., 2020, *The Limit Drawing Ratio in Die Angled Hydromechanical Deep Drawing Method*, Int. J. Adv. Manuf. Technol., 106/1–2, 791–801, https://doi.org/10.1007/s00170-019-04624-y.

[6] PHAN T., LUYEN T.T., NGUYEN D.T., 2023, *Applied Sciences a Study Utilizing Numerical Simulation and Experimental Analysis to Predict and Optimize Flange-Forming Force in Open-Die Forging of C45 Billet Tubes*, Applied Sciences, 13/16, https://doi.org/10.3390/app13169063.

[7] LUYEN T.T., PHAM Q.T., MAC T.B., BANH T.L., NGUYEN D.T., 2021, *Graphical Method Based on Modified Maximum Force Criterion to Indicate Forming Limit Curves of 22mnb5 Boron Steel Sheets At Elevated Temperatures*, J. Iron Steel Res. Int., 5, https://doi.org/10.1007/s42243-021-00567-5.

[8] LUYEN T.T., MAC T.B., NGUYEN D.T., 2023, *Simulation and Experimental Comparison Study Based on Predicting Forming Limit Curve of SUS304 Sheet Material*, Mod. Phys. Lett. B, 37/16, 1–7, https://doi.org/10.1142/S0217984923400018.

[9] FIRU A.C., TAPIRDEA A.I., FEIER A.I., DRAGHICI G., 2020, *Virtual Reality in the Automotive Field in Industry 4.0*, Mater. Today Proc., 45, 4177–4182, https://doi.org/10.1016/j.matpr.2020.12.037.

[10] MÜLLER M., WEISER I.F., HERRIG T., BERGS T., 2022, *Numerical Prediction of the Influence of Process Parameters and Process Set-Up on Damage Evolution During Deep Drawing of Rectangular Cups*, Eng. Proc., 26/1, https://doi.org/10.3390/engproc2022026006.

[11] ZAINAB A., MOHSEIN., WALEED H., JAWAD K., ASEEL H, 2023, *Experimental and Theoretical Analysis to Experimental and Theoretical Analysis to Produce Pentagonal Cup in Deep Drawing Process*, Production & Metallurgy Engineering, https://doi.org/10.30684/etj.2023.138865.1407.

[12] LI J., CHEN X., LIU X., 2021, *Investigation of Process Parameters and Plate Local Thickening on Residual Stresses in Hot Stamping Process*, Mech. Ind., 22, https://doi.org/10.1051/meca/2021015.

[13] CHEN K., CARTER A.J., KORKOLIS Y.P., 2022, *Flange Wrinkling in Deep-Drawing: Experiments, Simulations and a Reduced-Order Model*, J. Manuf. Mater. Process., 6/4, https://doi.org/10.3390/jmmp6040076.

[14] KARDAN M., PARVIZI A., ASKARI A., 2018, *Experimental and Finite Element Results for Optimization of Punch Force and Thickness Distribution in Deep Drawing Process*, Arab. J. Sci. Eng., 43/3, 1165–1175,

[15] MODANLOO V., HASANZADEH R., ESMAILI P., 2016, T*he Study of Deep Drawing of Brass-Steel Laminated Sheet Composite Using Taguchi Method*, Int. J. Eng. Trans. A Basics, 29/1, 103–108.

[16] AGARWAL E., CHATTERJI S., CHAKRAVORTY A., PADMANABHAN R., 2023, *Deep Drawing of Galvanized Plain Carbon Interstitial Free*, AIP Conf. Proc. 2788, 100002, https://doi.org/10.1063/5.0148689.

[17] MRABTI I.E., BOUZIANE K., TOUACHE A., HAKIMI A.E., CHAMAT A., DAYA A., 2023, *Effect of Process Parameters on the Deep Drawing Formability of Aluminum and Advanced High-Strength Steel Square Cups*, Int. J. Adv. Manuf. Technol., 124/5–6, 1827–1842, https://doi.org/10.1007/s00170-022-10616-2.

[18] TRAN M.T., SHAN Z., LEE H.W., KIM D.K., 2021, *Earing Reduction by Varying Blank Holding Force in Deep Drawing with Deep Neural Network*, Metals (Basel)., 11/3, 1–23, https://doi.org/10.3390/met11030395.

[19] SWIFT H.W., 1952, *Plastic Instability Under Plane Stress*, J. Mech. Phys. Solids, 1/1, 1–18, https://doi.org/10.1016/0022-5096(52)90002-1.

[20] GHAFAR A.A., ABDULLAH A.B., MAHMOOD J.I., 2021, *Experimental and Numerical Prediction on Square Cup Punch–Die Misalignment During the Deep Drawing process*, Int. J. Adv. Manuf. Technol., 113/1–2, 379–388, https://doi.org/10.1007/s00170-021-06595-5.

[21] HIBBITT, KARLSSON, SORENSEN, 2001, *ABAQUS / CAE User's Manual*, Ver. 6.10.1. ABAQUS Inc, 1–847.

[22] THE-THANH L., TIEN-LONG B., THE-VAN T., DUC-TOAN N., 2019, *A study on a deep-drawing process with two shaping states for a fuel-filter cup using combined simulation and experiment*, Adv. Mech. Eng., 11/8, 1–11, https://doi.org/10.1177/1687814019872674.

[23] TAGUCHI G., CHOWDHURY S., WU Y., TAGUCHI S., YANO H., 2005, *Taguchi's quality engineering handbook*, ASI Consult. Gr.